

For Reference

NOT TO BE TAKEN FROM THIS ROOM

Ex LIBRIS
UNIVERSITATIS
ALBERTAEASIS



THE UNIVERSITY OF ALBERTA

CURRENT SHEET TILT

IN A SHORT PARALLEL PLATE PLASMA ACCELERATOR

by



ROY E. DOWSWELL

A THESIS

SUBMITTED TO THE FACULTY OF GRADUATE STUDIES AND RESEARCH

IN PARTIAL FULFILMENT OF THE REQUIREMENTS FOR THE DEGREE

OF MASTER OF SCIENCE

DEPARTMENT OF ELECTRICAL ENGINEERING

EDMONTON, ALBERTA

SPRING, 1972

THE UNIVERSITY OF ALBERTA
FACULTY OF GRADUATE STUDIES AND RESEARCH

The undersigned certify that they have read, and recommend to the Faculty of Graduate Studies and Research, for acceptance, a thesis entitled "Current Sheet Tilt in a Short Parallel Plate Plasma Accelerator", submitted by Roy E. Dowswell in partial fulfilment of the requirements for the degree of Master of Science.

ABSTRACT

Magnetic induction and axial electric field strength were measured in a low density, short parallel plate, rail gun discharge. Current sheet tilt angles ranging from 19 degrees to 46 degrees were observed in helium and nitrogen at pressures from 0.07 torr to 0.75 torr. Tilt angle did not appear to be an obvious function of gas pressure. On the other hand, axial electric field strength seemed to affect the tilt angle since stronger field strength corresponded to weaker tilt. A negative axial electric field was observed in the current sheet region adjacent to the cathode. This negative field region increased monotonically with pressure and was much larger in nitrogen than in helium. The fraction of the discharge current carried by ions increased with pressure and was larger in nitrogen than in helium.

ACKNOWLEDGEMENTS

The author wishes to express his thanks to Dr. G. J. Pert for outlining and supervising the initial stages of this project. In addition the author wishes to thank Dr. P. R. Smy and Dr. A. A. Offenberger for supervising the completion of this project.

The author also wishes to thank the National Research Council of Canada and the Department of Electrical Engineering, University of Alberta, for financial support during this work.

Acknowledgement is also extended to the staff members and students of the Department of Electrical Engineering for their suggestions and cooperation.

TABLE OF CONTENTS

	Page
Chapter 1. INTRODUCTION	
1.1 Purpose of thesis	1
1.2 Scope of thesis	2
Chapter 2. EXPERIMENTAL CONDITIONS	
2.1 Apparatus	3
2.2 Operating conditions	6
Chapter 3. THEORETICAL AND EXPERIMENTAL MODELS	
3.1 Production of a current sheet	9
3.2 First theoretical model	9
3.3 Experimental observations	12
3.4 Advanced theoretical models	15
Chapter 4. EXPERIMENTAL RESULTS	
4.1 Validation of magnetic and electric probe diagnostics	17
4.2 Inductance of system	17
4.3 Magnetic induction and electric field strength measurements	18
Chapter 5. CONCLUSIONS AND SUGGESTIONS FOR FURTHER WORK	
5.1 Conclusions	36
5.2 Suggestions for further work	37
Appendix A MAGNETIC INDUCTION PROFILES	
A.1 Current strip model	38
Bibliography	41

LIST OF FIGURES

Figure		Page
2.1	Schematic diagram of a parallel plate plasma accelerator.	4
3.1	(a) Relative positions of electrodes, fields, and current sheet in the parallel plate plasma accelerator. (b) Reference frame used throughout this thesis.	10
3.2	Ion and electron orbits, in the reference frame of the moving current sheet, as they are reflected from the interface at the edge of the plasma.	11
4.1	Helium velocity measurements.	20
4.2	Nitrogen velocity measurements.	21
4.3	Relationship between gas pressure and current sheet velocity.	22
4.4	Helium magnetic induction profiles.	24
4.5	Helium magnetic induction profiles.	25
4.6	Nitrogen magnetic induction profiles.	26
4.7	Nitrogen magnetic induction profiles.	27
4.8	Helium electric field strength profiles.	30
4.9	Helium electric field strength profiles.	31
4.10	Nitrogen electric field strength profiles.	32
4.11	Nitrogen electric field strength profiles.	33
A.1	Collection of current strips simulating a current sheet.	38
A.2	Magnetic induction produced by current strips.	39
A.3	Magnetic induction profile for current strip model.	40
A.4	Typical magnetic induction oscilloscope trace.	40
 Table		
4.1	Parameters measured in the plasma accelerator.	19

LIST OF SYMBOLS

B	magnetic induction
t	time
R	resistance
L	inductance
C	capacitance
j	current density vector
<u>B</u>	magnetic induction vector
<u>E</u>	electric field strength vector
<u>v</u>	velocity vector
I	current
x,y,z	three coordinate axes
θ	cylindrical coordinate axis
Ey	electric field strength componant along y axis
Bz	magnetic induction componant along z axis
w _{be}	electron cyclotron frequency
t _{ce}	electron collision period

CHAPTER 1

INTRODUCTION

1.1 Purpose of thesis

In 1956 Rosenbluth¹ presented a theoretical study of the dynamics of an electrically pinched gas [see chapter 3]. His model indicated that a very fast moving sheath of plasma could be created by a magnetically driven shock wave. It was originally hoped that such a scheme could produce sufficient densities and temperatures to be of thermonuclear interest. Experimental results have so far not born this out.

However, magnetically driven shock waves have many other uses. The hot, dense plasma produced in these devices can be used for many basic plasma investigations. They are used extensively for shock wave studies. Various rocket propulsion systems have been designed and studied which use an electromagnetically accelerated plasma for thrust. And more recently it has been suggested that an electromagnetic plasma gun could be used as a neutral gas injector for stabilizing a fusion device².

Although electromagnetically produced shock waves have many promising uses, very little is known about the structure of the shock wave itself. In particular, a model explaining all of the phenomena occurring in the current sheet, which drives the shock in a plasma accelerator, has not yet been developed. One such phenomenon is the tilting of the current sheet so that the part of the current sheet nearest the anode of the accelerator travels ahead of the current sheet nearest the cathode.

The purpose of this thesis is to investigate the tilt in the current sheet in a short parallel plate plasma accelerator as a function of pressure and gas type. The region investigated is that of low pressure [0.07 - 0.75 torr], resulting in current sheet speeds centered around 6 cm/ μ sec. This velocity range was chosen because a variation in tilt with pressure had been found in hydrogen in this region^{3,4}.

1.2 Scope of thesis

This thesis is an extension of work carried out by Lovberg^{5,6} and Pert^{3,4} on the structure of a current sheet formed in a short parallel plate plasma accelerator. Pert^{3,4} found a transition between a perpendicular and a tilted current sheet to occur at about 0.3 torr in hydrogen. A similar transition was expected in helium and nitrogen in this pressure region.

Electric field strength and magnetic induction were measured in the current sheet with a floating dual-electrode electrostatic probe and a small radius coil magnetic probe. Magnetic induction profiles show the shape of the current sheet and thus illustrate the tilt [see Appendix A]. Electric field strength profiles indicate whether the ions present in the sheet were accelerated by the electric field or by the magnetic field. If the electric field strength was insufficient to accelerate the ions to current sheet velocity then they must have been accelerated by the magnetic induction. Electric field strength profiles have not previously been recorded. Hopefully they will shed more light onto the microstructure of the current sheet.

CHAPTER 2

EXPERIMENTAL CONDITIONS

2.1 Apparatus

The experimental apparatus consisted of a short parallel plate plasma accelerator placed inside a vacuum chamber with ports for probing along three axes. An energy storage capacitor was connected to the accelerator electrodes via a thyratron triggered spark gap. Magnetic and electrostatic probes were inserted through the ports into the gun. An oscilloscope was used to monitor all signals. Figure 2.1 schematically represents the experimental apparatus.

Two, polished-flat, stainless-steel plates were used for the electrodes of the accelerator. They were mounted on a flat piece of 1/4 in. thick pyrex glass with a separation of 2.5 cm between their adjacent faces. The electrodes were 8 cm wide, 7.5 cm long and 0.6 cm thick. A 0.8 cm diameter hole was drilled on the centerline, 4.4 cm from the back-plate through the top electrode, to allow the insertion of a probe into the current sheet. Thin teflon bushings separated the electrodes from the back-plate, and back-plate from the end plate of the vacuum chamber.

The vacuum chamber was 15 cm in diameter and 13 cm long, constructed from stainless-steel with a pyrex glass end plate. Ports were placed in the vacuum chamber to allow probing from the top, side, and muzzle end of the plasma gun. These three probing axes intersected midway between the top and bottom electrodes, midway from side to side

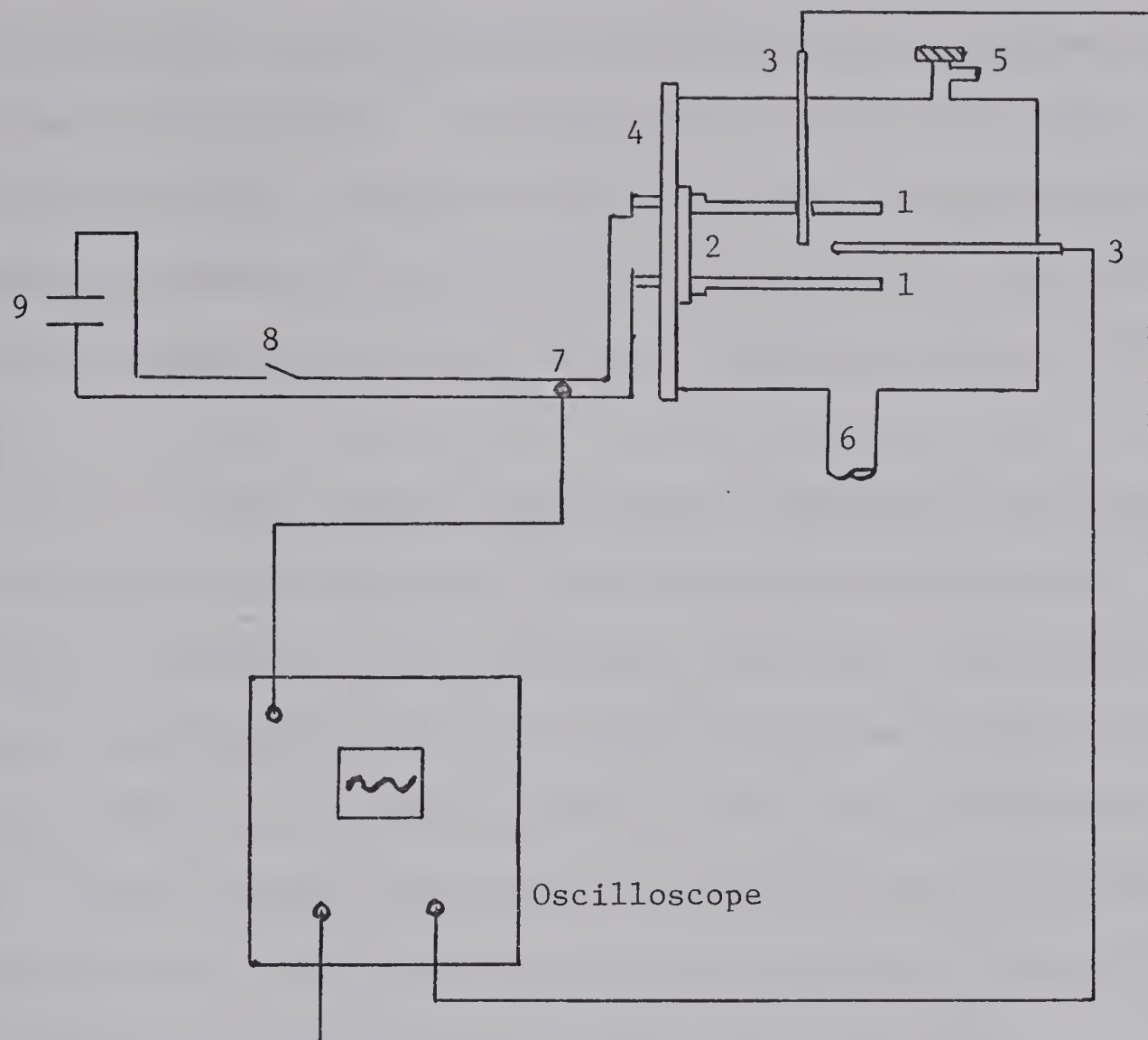


Figure 2.1 Schematic diagram of a parallel plate plasma accelerator.

1. Accelerator electrodes
2. Accelerator back-plate
3. Probes
4. Vacuum chamber end plate
5. Gas inlet
6. Connecting pipe to vacuum pump
7. Rogowski coil
8. Thyatron triggered spark gap
9. Energy storage capacitor

of the plasma gun and 4.4 cm from the back-plate end of the gun. Thus the current sheet could be completely probed from top to bottom, side to side and front to back. Gas was metered into the top of the vacuum chamber and pumped out the bottom. A mercury vapour diffusion pump with a nitrogen filled cold trap, pumping in conjunction with a roughing pump could maintain a pressure of one micro-torr in this system. Gas pressure inside the chamber was monitored with an ionization guage and Pirani guage.

A 14.5 μF energy storage capacitor was connected to the plasma gun via a spark gap switch and a low inductance short parallel plate transmission line bolted onto the accelerator electrodes. Thin sheets of mylar separated the two 3.5 in. wide copper leads used for the transmission line. The three electrode spark gap switch was a swinging cascade type. A direct current power supply charged the capacitor through a 100 k ohm resistor. The charging current was limited to 40 mA and the voltage, limited to 20 kV, was monitored with a DC volt meter.

Magnetic induction present in the current sheet was measured with standard magnetic probes of the type described by Lovberg⁷. They had 20 turns of 46 guage copper wire wound on a 0.9 mm diameter air core. The leads, which were twisted to shield against unwanted magnetic pickup and to form a low inductance pair, were connected to a subminiature coaxial cable. A 0.4 cm diameter sealed quartz glass tube, which was inserted through a probing port into the space between the accelerator electrodes, surrounded the coil. Passive integration of the probe signal produced the desired magnetic induction since the emf induced on the probe coil was proportional to dB/dt . Magnetic probes were calibrated

using a signal obtained from a known 0.33 MHz oscillating magnetic field. This reference field was created by discharging a small capacitor through an air core solenoid. Measured values of voltage and current for the solenoid determined the magnitude of this field.

Electric field strength in the plasma was measured with a differential-field probe described by Lovberg⁷. The probe used was identical in design to that used by Pert⁴. It was a screened two-pin probe encased in 0.6 cm diameter quartz glass tubing with tungsten wire electrodes 0.2 cm long and separated by 0.15 cm. The leads were twisted and shielded and connected to two subminiature coaxial cables which led to a differential transformer. This screened common mode rejection transformer had 23 turns resulting in a bandwidth of 2.6 MHz.

Throughout the experiment a dual beam Tektronix 556 oscilloscope was used to display the probe signals. It had an adequate bandwidth for all signals produced by the probes. A Rogowski coil was positioned between the external leads providing a signal to externally trigger the oscilloscope.

2.2 Operating conditions

To ensure a clean environment for the plasma accelerator to operate in, the vacuum chamber was pumped down to a pressure of 10^{-6} torr before measurements were made. In addition, the plasma gun first had to be fired several times in succession to reduce the amount of absorbed gas on the back-plate and electrodes to an equilibrium level. Once this was accomplished the current sheet was very reproducible from shot to shot.

The plasma accelerator was fired with gas continuously flowing through the vacuum chamber. No gas injection system was employed. Enough time elapsed between firings of the plasma gun to allow the back-

ground gas to be replaced by a fresh supply.

For all measurements of the current sheet the capacitor was charged to 16 kV before firing. Measurements were only taken during the first half cycle of the discharge.

Current sheets were probed in helium with background pressures of 0.1, 0.25, 0.5, and 0.75 torr and nitrogen at 0.07, 0.1, 0.3, and 0.5 torr.

All sets of data were obtained by making two passes along a probing axis. For example measurements were made at points on the vertical axis starting at the topmost position and working down to the lowest position, then progressing back up to the top. This was done to ensure that the current sheet parameters did not vary in time from the beginning to the end of a data set. In addition, a magnetic probe signal from the edge of the current sheet was always recorded simultaneously with each measurement. If this reference signal was constant then it was assumed that the current sheet was reproducible throughout the data set. Two measurements from successive firings were recorded on the same photograph to further ensure that reproducibility of the current sheet was occurring.

Measurements of magnetic induction and electric field strength in the current sheet were taken as the current sheet travelled past the probes, that is, all measurements were taken as a function of time at constant position. Thus a spatial picture of the current sheet at one time was not obtained, but rather a one dimensional spatial picture as it varied with time was plotted. Because of this diagnostic method caution should be emphasized when interpreting the results. A simple velocity transformation to obtain a spatial picture of the current sheet

may not be completely accurate since the total current flowing through the current sheet varied slightly during the measurement time. This variation in total current was due to the underdamped R-L-C oscillation of the discharge. Measurements, taken over 1/8 of the period of oscillation, were centered on the first peak of the discharge current.

CHAPTER 3

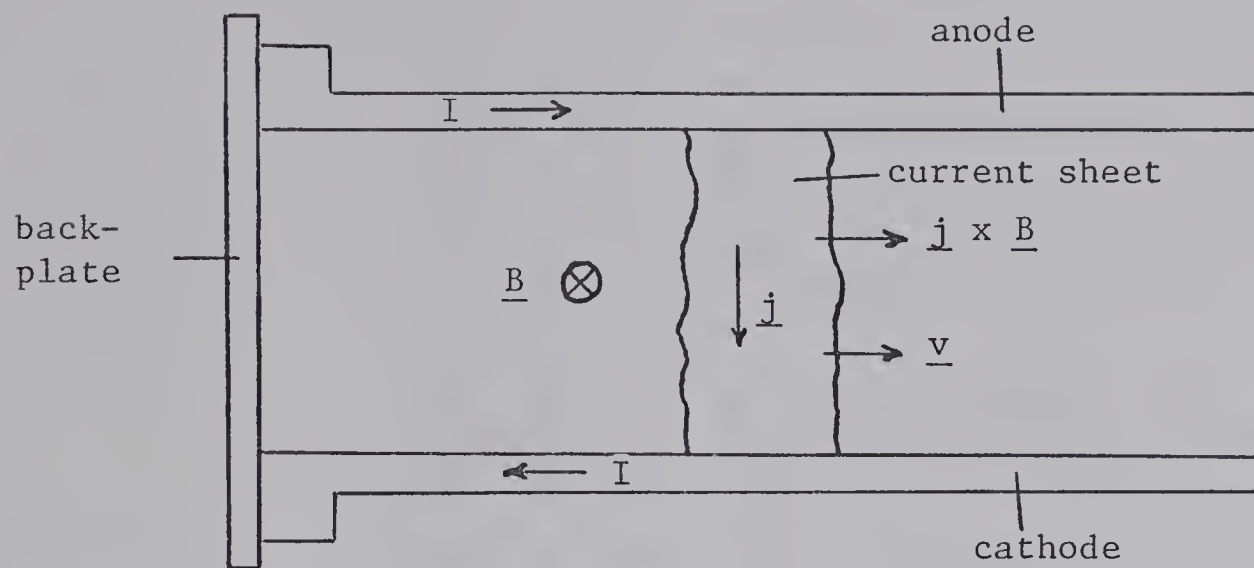
THEORETICAL AND EXPERIMENTAL MODELS

3.1 Production of a current sheet

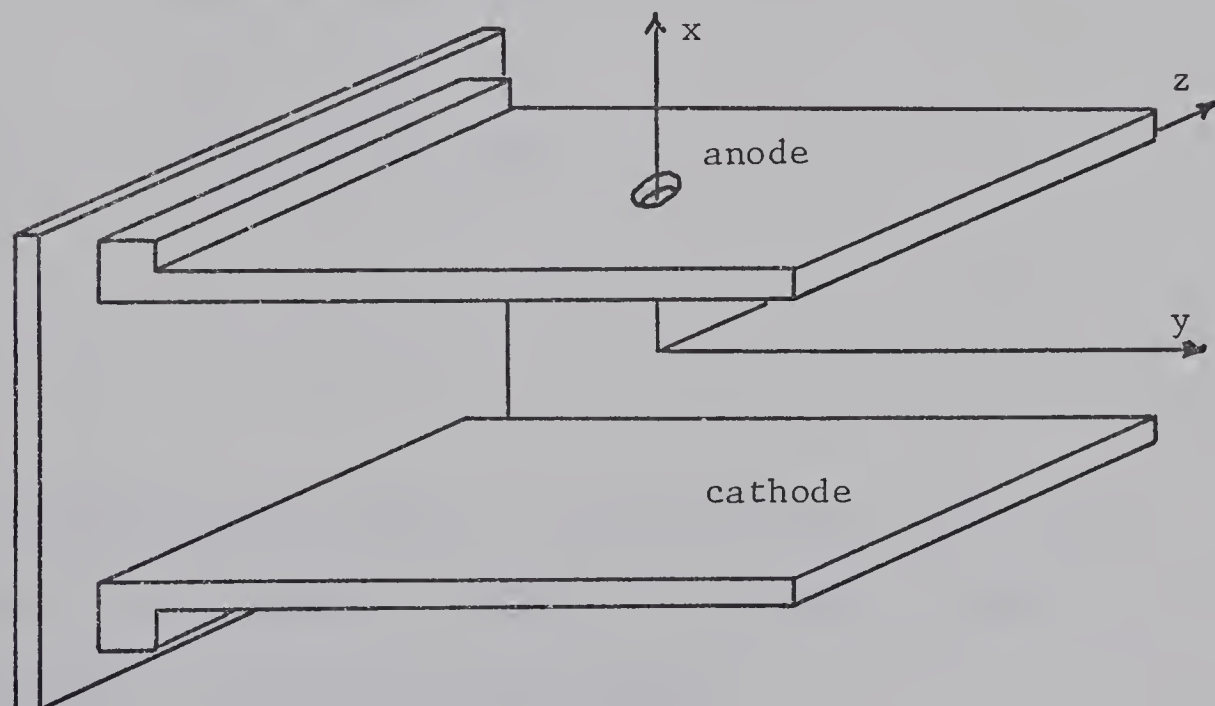
Gaseous breakdown between two electrodes of a parallel plate plasma accelerator produces a current sheet. Tracking along the face of the back-plate starts the breakdown. The magnetic field produced by this breakdown current interacts with the current carriers to form a $\underline{j} \times \underline{B}$ force on the current sheet, accelerating it away from the back-plate. Figure 3.1 indicates the relative positions and directions of electrodes, fields, and current sheet as well as a reference frame to be used throughout the discussion.

3.2 First theoretical model

In 1956 Rosenbluth¹ discussed the feasibility of accelerating a plasma with a propagating current sheet. His model - based on the assumptions that the current sheet propagated with a velocity large compared to the thermal velocity of the plasma into a non-magnetized, fully ionized plasma - indicated that all particles coming into contact with the current sheet would be reflected by the magnetic field, provided that no particle collisions took place during the contact [see figure 3.2]. That is, a charged particle which travelled into a magnetic field region would be turned about by the cyclotron effect and leave the region in the opposite direction. Furthermore, the plasma was taken to be a perfect conductor with a thin current sheet on its surface which separated the plasma from the magnetic field region. A space charge electric field



(a)



(b)

Figure 3.1 (a) Relative positions of electrodes, fields, and current sheet in the parallel plate plasma accelerator.
 (b) Reference frame used throughout this thesis.

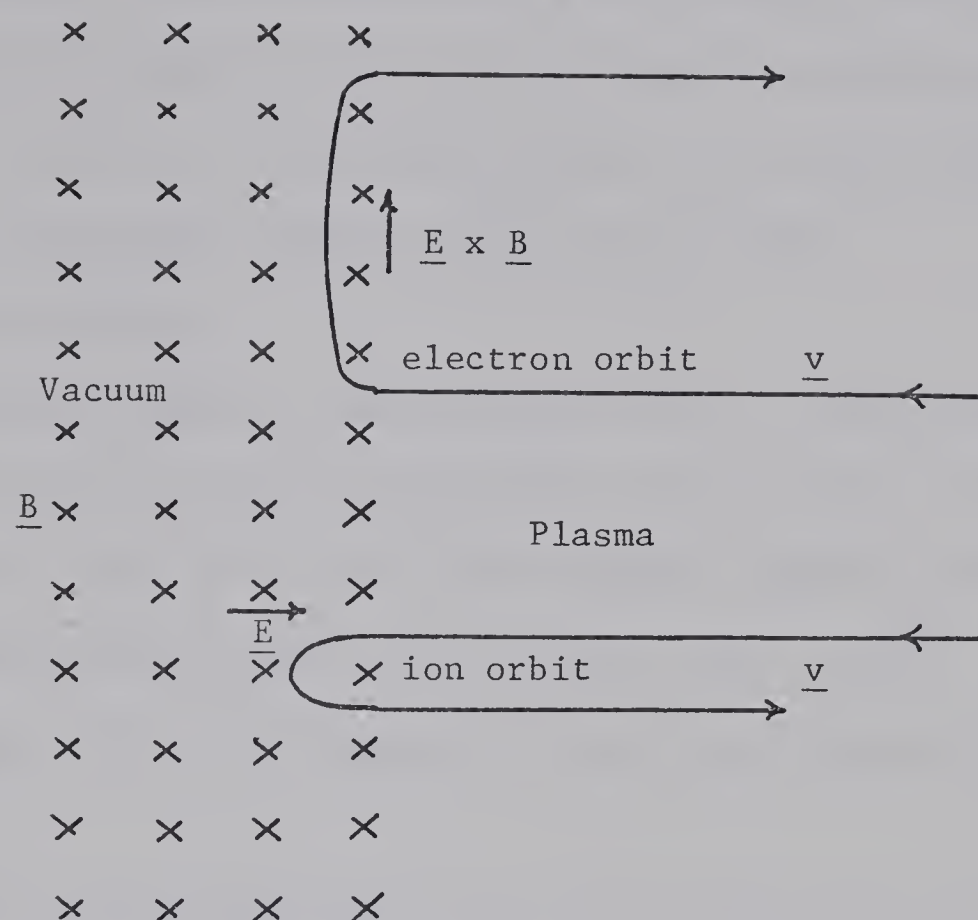


Figure 3.2 Ion and electron orbits, in the reference frame of the moving current sheet, as they are reflected from the interface at the edge of the plasma.

was produced in the magnetic field region since the ions which had a larger radius of gyration penetrated further into the magnetic field region than the electrons. The ions described a very shallow orbit since they were accelerated far more by the electric field than the magnetic field. On the other hand, the electrons underwent a very wide orbit since they gained considerable momentum from an $\underline{E} \times \underline{B}$ drift.

3.3 Experimental observations

A considerable amount of experimental work has been carried out since Rosenbluth first proposed the method of accelerating a plasma with a current sheet. Much of this has been directed towards gaining an understanding of the microstructure of the current sheet itself. A brief summary of some of the more important results is presented in this section.

Experimental observation showed that all current sheets had a width varying from less than 1 cm to 3 or 4 cm depending on gas type and pressure. The assumption of a thin current sheet separating the magnetic field region from the plasma could not be used therefore, to describe these current sheets.

However, as Rosenbluth hypothesized, the observed current sheets acted as efficient pistons snowplowing the bulk of the gas to current sheet speed. Lovberg^{5,6} and Pert³ reported efficient snowplowing in hydrogen at 0.35 and 0.1 torr respectively. Burton and Jahn⁸ found that 96% of the gas was swept up by a current sheet propagating into argon at 0.12 torr. One exception was found in 0.5 torr of hydrogen by Pert⁴. The current sheet was not an efficient piston since gas bubbles were found which had detatched themselves from the rear of the current sheet.

Rosenbluth's model predicted acceleration of ions by a space charge electric field E_y . In several instances the measured E_y was insufficient to accelerate the ions to current sheet speed. Lovberg⁵ found E_y throughout most of the current sheet to be ten times smaller than required to accelerate the ions in hydrogen at 0.3 torr. However, near the cathode he found that E_y rose to a sufficient value to accelerate the ions to current sheet speed. Burton and Jahn⁸ measured E_y in argon at 0.12 torr to be large enough to provide only one half of the energy that an ion, travelling at current sheet speed, would have. In hydrogen at 0.5 torr Pert⁴ found that E_y was negative in the front region of the current sheet. This negative E_y would accelerate ions in the opposite direction to the current sheet. However, Lovberg⁵ using nitrogen at 0.09 torr and Pert³ using hydrogen at 0.1 torr found a sufficiently large E_y to accelerate the ions to the speed of the current sheet.

Inconsistencies in observed values of E_y led to differing opinions on the identity of the current carrier in the current sheet. Lovberg⁵ with hydrogen at 0.35 torr, Johannson⁹ with hydrogen at 0.1 torr and nitrogen at 0.05, 0.1, and 0.4 torr and Burton and Jahn⁸ with argon at 0.12 torr, attributed a large portion of the current to the ions. Ion displacement current, hypothesized Lovberg⁵, was responsible for most of the current flow. Burton and Jahn⁸ said that since E_y was insufficient to accelerate the ions they were accelerated by a $j \times \underline{B}$ force, hence they carried a large fraction of the current. Sufficient ions, Johannson⁹ claimed, were funneled to the cathode to carry all of the current due to a tilt in the shock wave accompanying the current sheet. Similarly, Lovberg⁵ maintained that since E_y was large enough to accelerate the ions

to current sheet speed in nitrogen at 0.09 torr the current was carried by electrons. Pert³ found that E_y was sufficient to drive all of the current in the sheet through an $\underline{E} \times \underline{B}$ drift of the electrons towards the anode.

The model of Rosenbluth assumes the current sheet to be planar and perpendicular to the current sheet velocity. Some authors have experimentally found this to be the case, others have observed an irregular shaped current sheet and a tilted current sheet. No tilt was observed by Lovberg^{5,6} in hydrogen at 0.35 and 0.3 torr. Burton and Jahn⁸ found a slight tilt [3° to 5°] in argon at 0.12 torr and Pert³ found the bulk of the current sheet in hydrogen at 0.1 torr to be perpendicular to the electrodes. However, at 0.5 torr of hydrogen Pert⁴ found that the bulk of the current flow was inclined to the electrode perpendicular. An inclination of about 30° was observed in nitrogen at 0.12 torr by Lovberg⁶ and Johansson⁹ using hydrogen at 0.1 torr and argon at 0.05, 0.1, and 0.4 torr found the current sheet to be tilted anywhere from 30° to 50° . Furthermore this observed tilt did not vary systematically with gas pressure. In all of these cases the current sheet was tilted such that the portion nearest the anode travelled ahead of that portion nearest the cathode.

It should be noted that all of the plasma accelerators used to obtain the previously described results were designed to create a magnetic field which would not vary in the z direction or correspondingly in the ϕ direction for cylindrical type discharges. Lovberg⁵ found the current sheet in hydrogen at 0.35 torr not to vary with z over the central region and similarly Pert³, with hydrogen at 0.1 torr, observed the magnetic field to be constant with z at the midplane of the current sheet.

In the above cases the current sheet velocity varied from 4 cm/ μ sec to 8 cm/ μ sec.

Evidently experimental inconsistencies exist between results reported by different authors. A wide range of tilt angles have been observed and many different values for E_y have been measured which have led to varied opinions on current partitioning between ions and electrons.

3.4 Advanced theoretical models

Since Rosenbluth's model is inadequate to describe the complicated current sheet structures observed experimentally, several authors have developed more elaborate mathematical models which predict some of the observed details of the current sheet.

Khizhnyak and Kalmykov¹⁰ have shown that an oscillating electric field could be generated leading to closed current loops behind the current sheet. Using the equations of motion describing a charged particle's orbit, Kulinski¹¹ has shown that charged particles can be reflected by, trapped in, or pass through a current sheet. Pert^{12,13} has examined the current sheet structure under steady-state conditions for two regimes, the first being an ionizing current layer propagating into a cold non-ionized gas using a collision-free approximation. He also examined a singly ionizing current sheet matching a collisionless model for the front of the sheet to a collision-dominated magnetohydrodynamic two-fluid calculation for the back of the sheet.

Unfortunately these models do not incorporate a tilt in the current sheet or predict the occurrence of one. However, several authors have conjectured possible reasons for the tilt but so far none have produced a mathematical model with tilt. Pert⁴ attributed the tilt to an

electron Hall parameter of about unity. Kvartskhava, et. al.¹⁴ say the tilt is caused by sputtering of ions from the cathode. The emitted ions constitute a local current in the opposite direction thus they are accelerated in the opposite direction to the bulk of the current sheet, retarding the forward motion of the sheet near the cathode.

In the following chapter experimental observations are reported in an attempt to elucidate the tilting phenomenon of the current sheet.

CHAPTER 4

EXPERIMENTAL RESULTS

4.1 Validation of magnetic and electric probe diagnostics

Various tests were performed on the probes while they were in the current sheet to ensure that stray magnetic or electric pick-up was negligible. A substantial magnetic induction was observed only in the z direction. Any other orientation of the magnetic probe resulted in negligible signal which implied that electrostatic pick-up by the probe was small. Screening due to boil-off of the glass tube appeared to be negligible since the magnetic induction measured was independent of the alignment of the probe shaft with the three probing axes. This independence also indicated that unwanted magnetic pick-up was not recorded. In addition, the signal from a probe was not altered when another probe was brought into the vicinity of the current sheet implying that the probe did not alter the magnetic induction appreciably.

Effective magnetic screening of the electrostatic probe was shown by a negligible measured field in the z direction. It was assumed that spatial differences in electron thermal energy were small so differences in floating potential were taken to be equivalent to differences in plasma potential between two points in the current sheet [see Lovberg⁷]. Thus the measured voltage was used directly to calculate the electric field in the current sheet.

4.2 Inductance of system

The period of the total current oscillation was measured to be

8.6 μ s. This oscillation decayed to 1/e of its original magnitude in about 4 oscillations. Assuming the plasma gun, connecting leads, and capacitor to be a series R-L-C circuit with the 14.5 μ F energy storage capacitor charged to 16 kV, the inductance, resistance and peak current can be found. The calculated values were as follows: inductance - 0.13 μ H, resistance - 7.5×10^{-3} ohm, peak current - 158 kA.

4.3 Magnetic induction and electric field strength measurements

Horizontal probing at points along the z axis indicated the current sheet to be flat and parallel to the back-plate for a width of 6 cm in helium and 4 cm in nitrogen. This flat parallel region was centered on the y axis. In both helium and nitrogen the current density was less at the outside edges of the current sheet than in the middle flat region. Lovberg⁵ and Pert³ reported finding a flat parallel region with respect to the z axis as well.

Table 4.1 summarizes the parameters measured in the plasma accelerator. A maximum error is indicated for the value of each parameter. The following paragraphs describe the method used for obtaining the values as well as the significance of them.

Current sheet velocity was determined by plotting time of arrival of two different magnitudes of magnetic induction at various points along the y axis. Figures 4.1 and 4.2 display the results for helium and nitrogen respectively at the four pressures used for each. There was some discrepancy between velocity of the first part of the current sheet and velocity of the second. This can be attributed to an expanding or contracting of the current sheet and an average of the two values gives a fairly accurate velocity for the current sheet. Each

<u>GAS</u>	<u>PRESSURE</u>	<u>CAPACITOR VOLTAGE</u>	<u>CURRENT SHEET VEL.</u>	<u>FILLING DENSITY</u>
	torr $\pm 10\%$	kV $\pm 10\%$	cm/ μ s $\pm 15\%$	10^{15} atoms/cm 3 $\pm 12\%$
He	0.1	16	7.1	3.2
He	0.25	16	6.7	8.0
He	0.5	16	6.2	16.0
He	0.75	16	5.8	24.0
N ₂	0.07	16	6.9	4.5
N ₂	0.1	16	5.6	6.4
N ₂	0.3	16	4.3	19.3
N ₂	0.5	16	3.3	32.2
 <u>SHEET WIDTH AT x = 0</u>				
	cm $\pm 20\%$	<u>B_z RANGE</u>	<u>E_y RANGE</u>	<u>TILT ANGLE</u>
		weber/m 2 $\pm 10\%$	10^3 volts/m $\pm 10\%$	degrees $\pm 35\%$
		<u>from</u> <u>to</u>	<u>from</u> <u>to</u>	
	6.2	0.13 0.78	-16.0 26.7	27
	4.9	0.13 0.78	-10.7 32.0	46
	4.6	0.13 0.78	-16.0 32.0	34
	4.9	0.13 0.78	-21.3 32.0	38
	7.4	0.13 0.78	-26.7 21.3	19
	6.0	0.13 0.78	-21.3 21.3	31
	0.9	0.13 0.78	-26.7 26.7	39
	0.6	0.13 0.78	-32.0 10.7	22

Table 4.1 Parameters measured in the plasma accelerator.

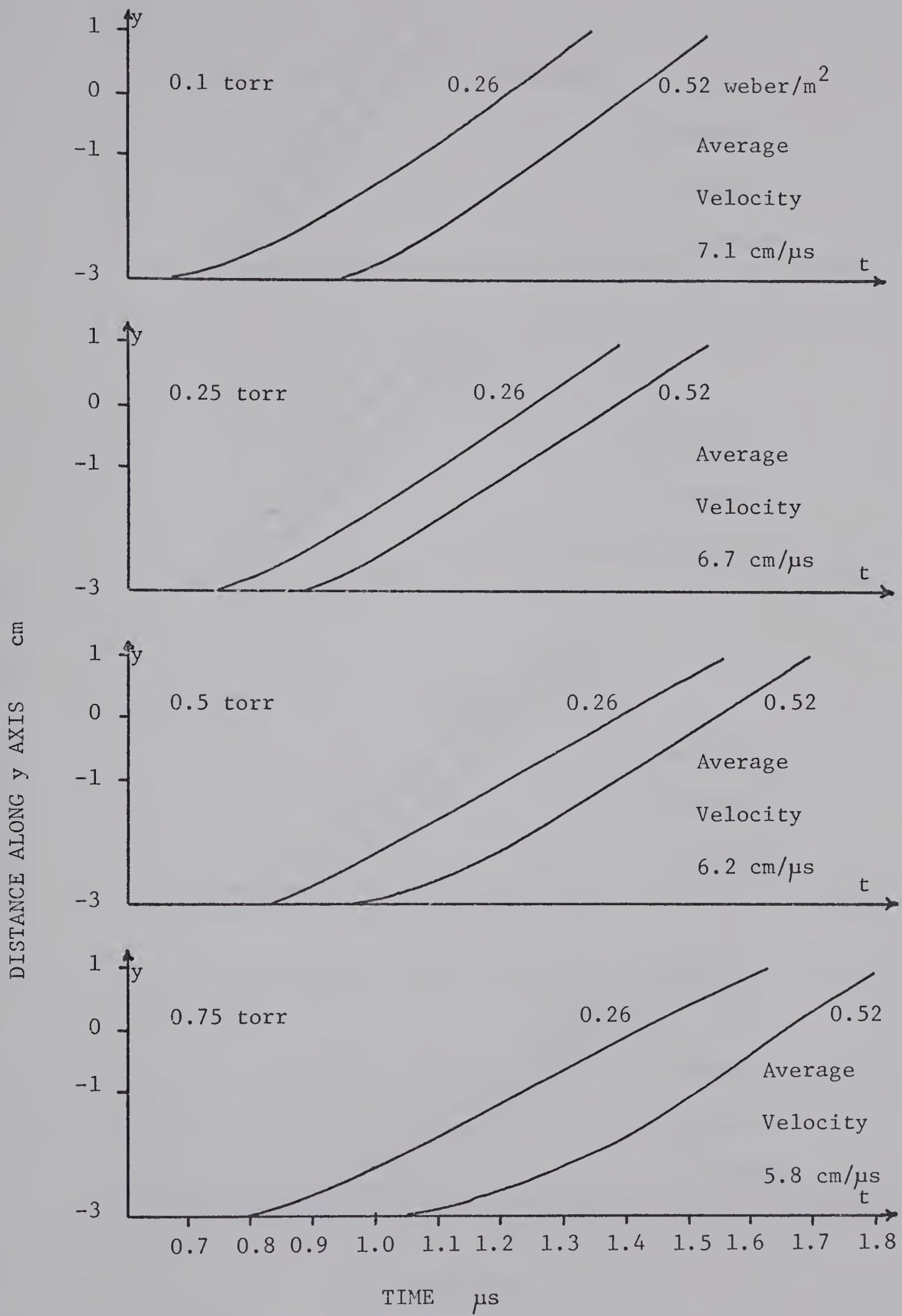


Figure 4.1 Helium velocity measurements.

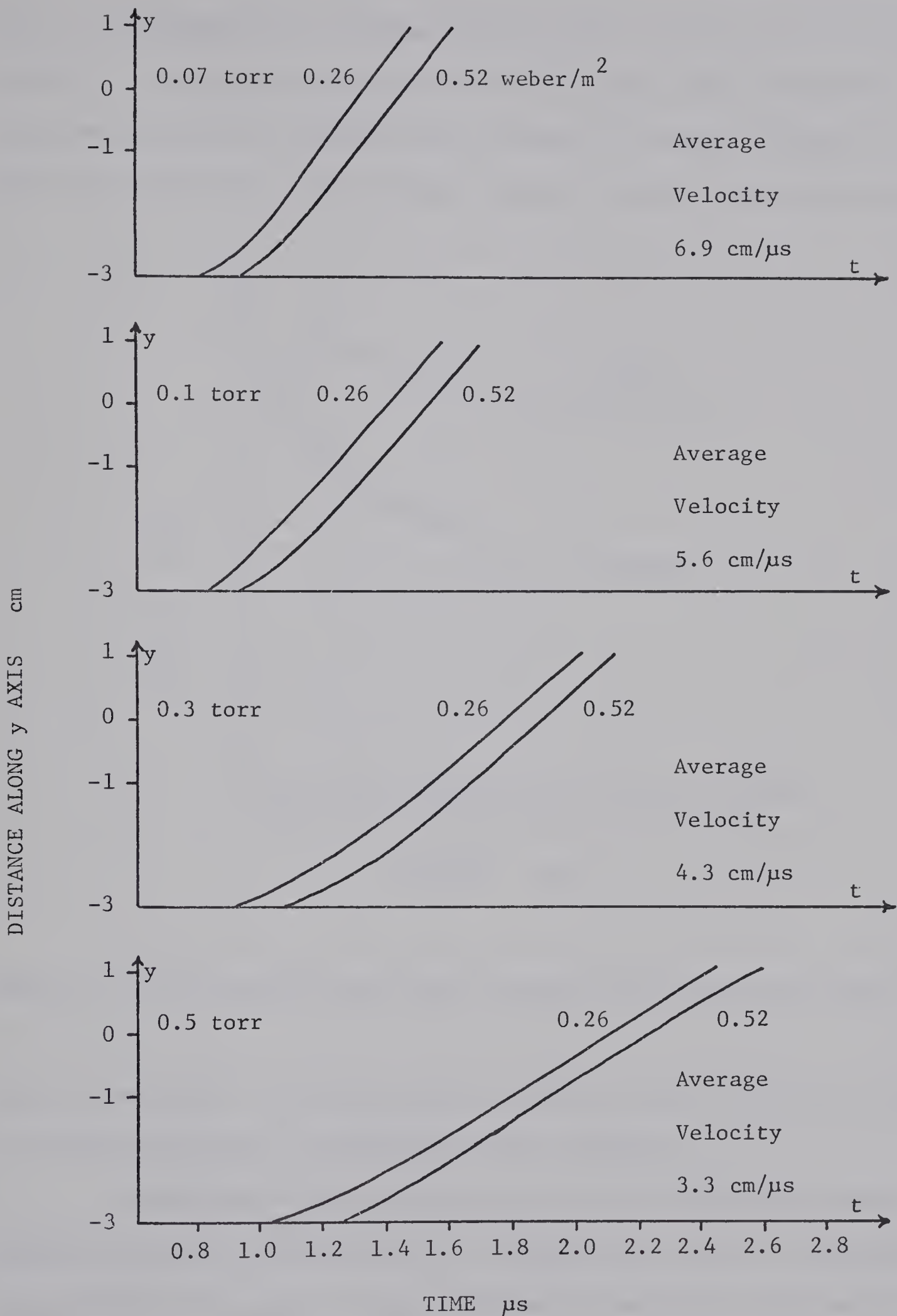


Figure 4.2 Nitrogen velocity measurements.

plot is accompanied by an average velocity value which is also listed in table 4.1. A pressure dependence on velocity was quite evident with an increase in pressure resulting in a decrease in velocity. Figure 4.3 shows this dependence. The velocity varies linearly with pressure over

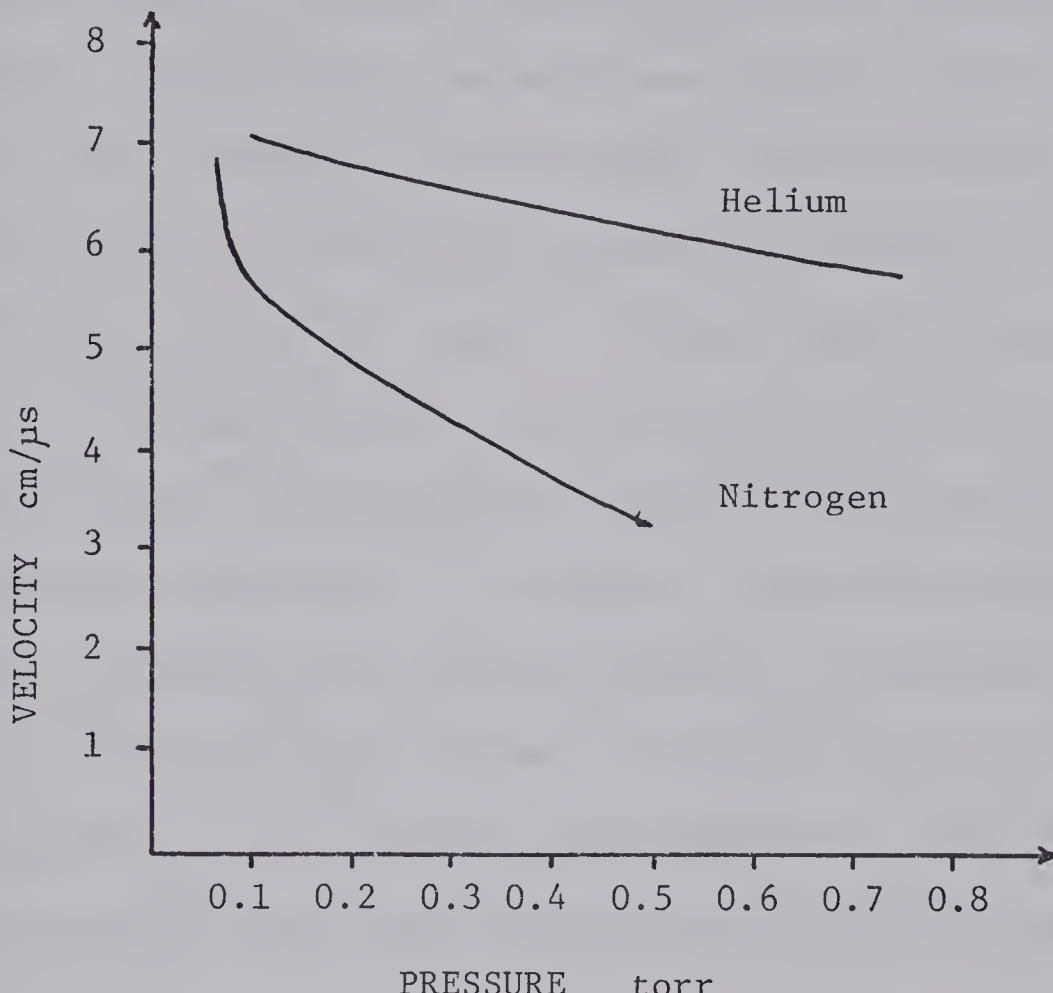


Figure 4.3 Relationship between gas pressure and current sheet velocity.

most of the region. For low pressure, however, there is a large increase in velocity resulting in a departure from linearity.

Background filling density was calculated from the pressure readings using the ideal gas law for a temperature of 80° F. Nitrogen, being diatomic, has twice as many atoms/cm³ as helium for the same pressure.

Current sheet width was calculated at $x = 0$ and $z = 0$ by multiplying the difference in arrival time of the front and the rear of the current sheet at $y = 0$ by the average current sheet velocity. The arrival times were taken from figures 4.4 to 4.7 which are magnetic induction profiles in the $x - t$ frame. These figures are discussed in the next paragraph. A value of 0.13 weber/m^2 was used for the front of the current sheet and 0.78 weber/m^2 for the rear. The 0.0 weber/m^2 value was not used since it was difficult to ascertain its position due to noise on the first part of the signal. Current density decreased sharply beyond the 0.78 weber/m^2 profile line so it was taken as the rear cut-off for the sheet. In nitrogen for the two highest pressures 0.65 weber/m^2 was used for the rear of the sheet. A pressure dependence is again evident. Increasing the pressure results in a decrease in current sheet width. This is much more evident in nitrogen than in helium since nitrogen ranges from a very diffuse current sheet to a very compact sheet, whereas helium stays quite diffuse over the entire pressure range.

Figures 4.4 to 4.7 were plotted to indicate the shape of the current sheets and more specifically the tilt of the current sheets. They show the magnetic induction at $y = 0$ and $z = 0$ for various x and t values for the four pressures used in both helium and nitrogen. The current sheets in helium at each pressure and nitrogen at the two lowest pressures are extremely diffuse and irregular in shape as shown by figures 4.4 to 4.6. With current sheets of this type it is very difficult and probably meaningless to specify a tilt angle for the sheet since the angle of the tilt varies throughout the current sheet. The tilt angle

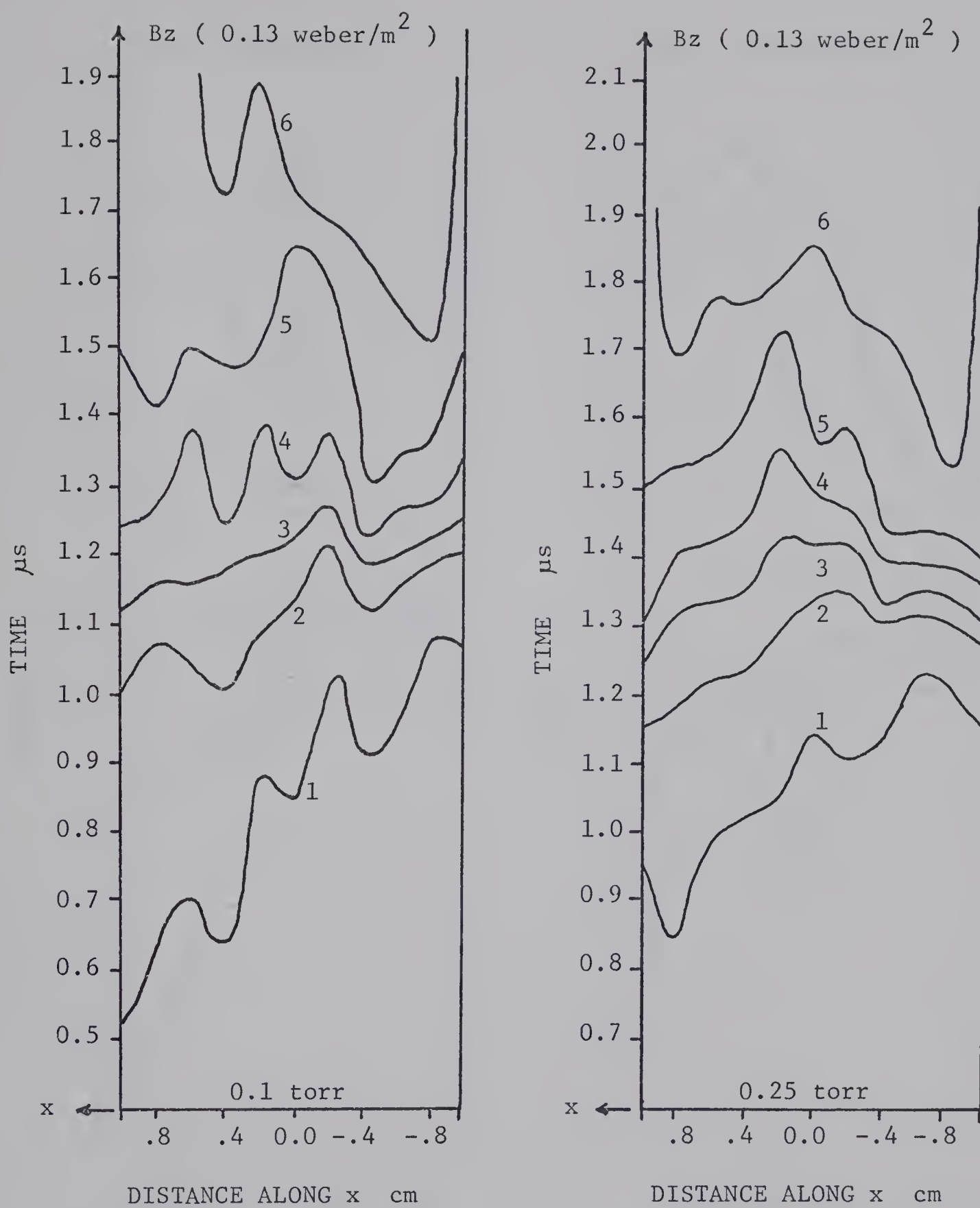


Figure 4.4 Helium magnetic induction profiles.

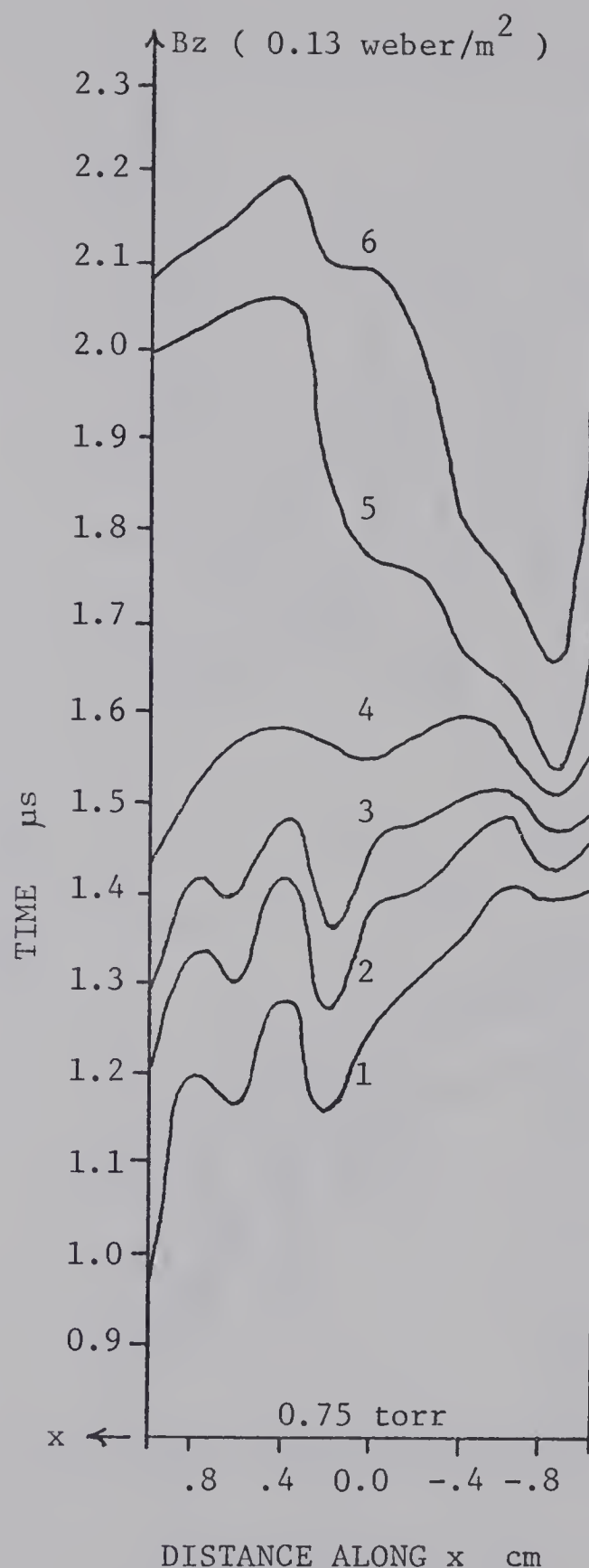
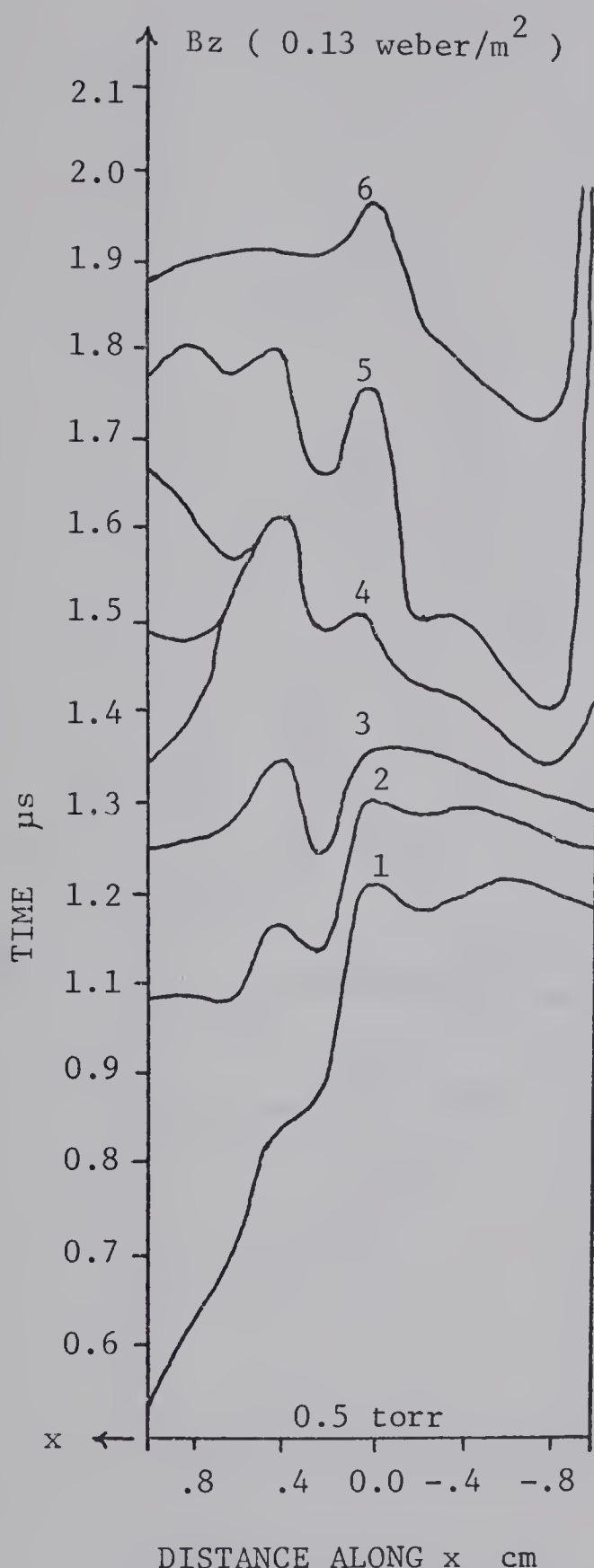


Figure 4.5 Helium magnetic induction profiles.

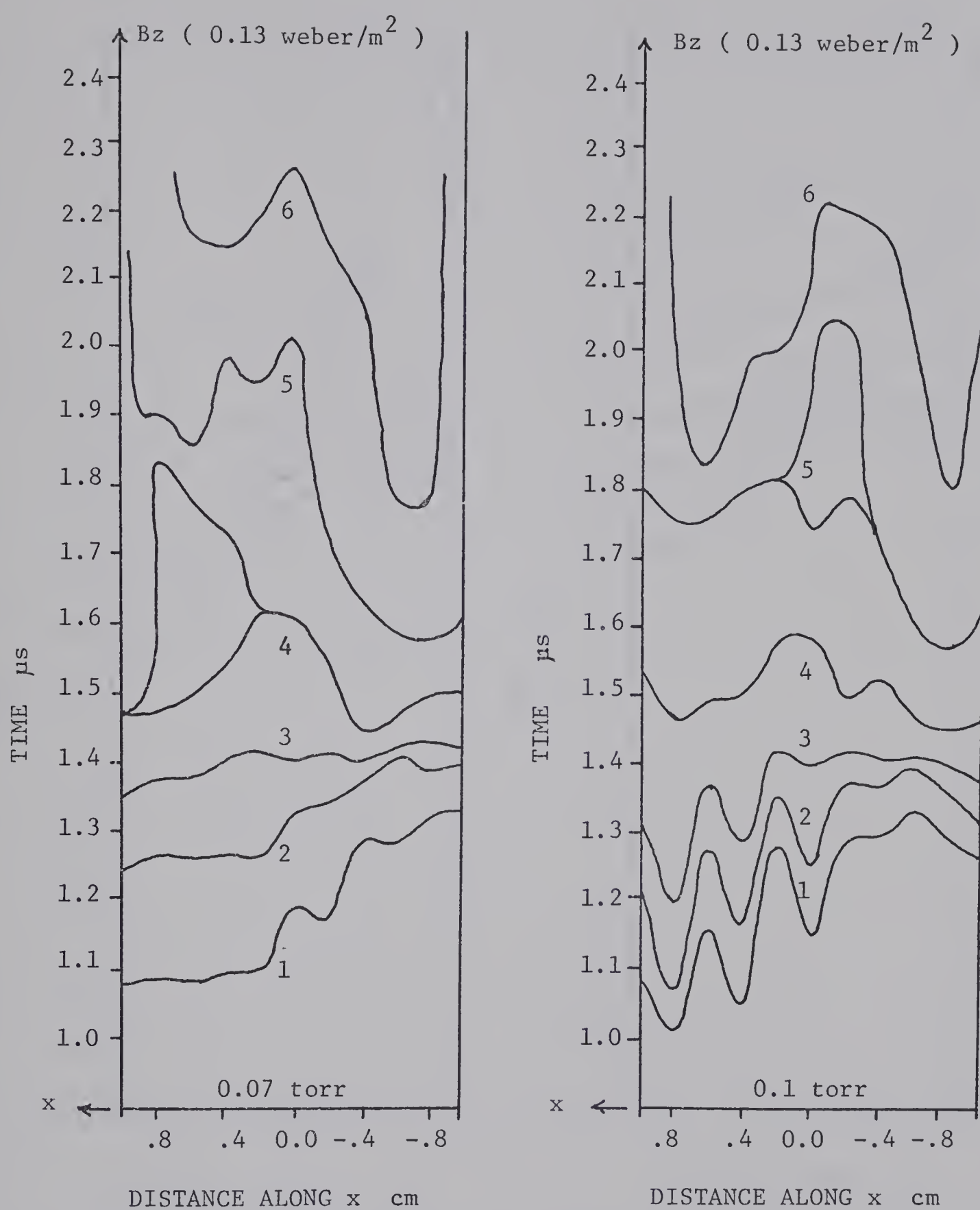


Figure 4.6 Nitrogen magnetic induction profiles.

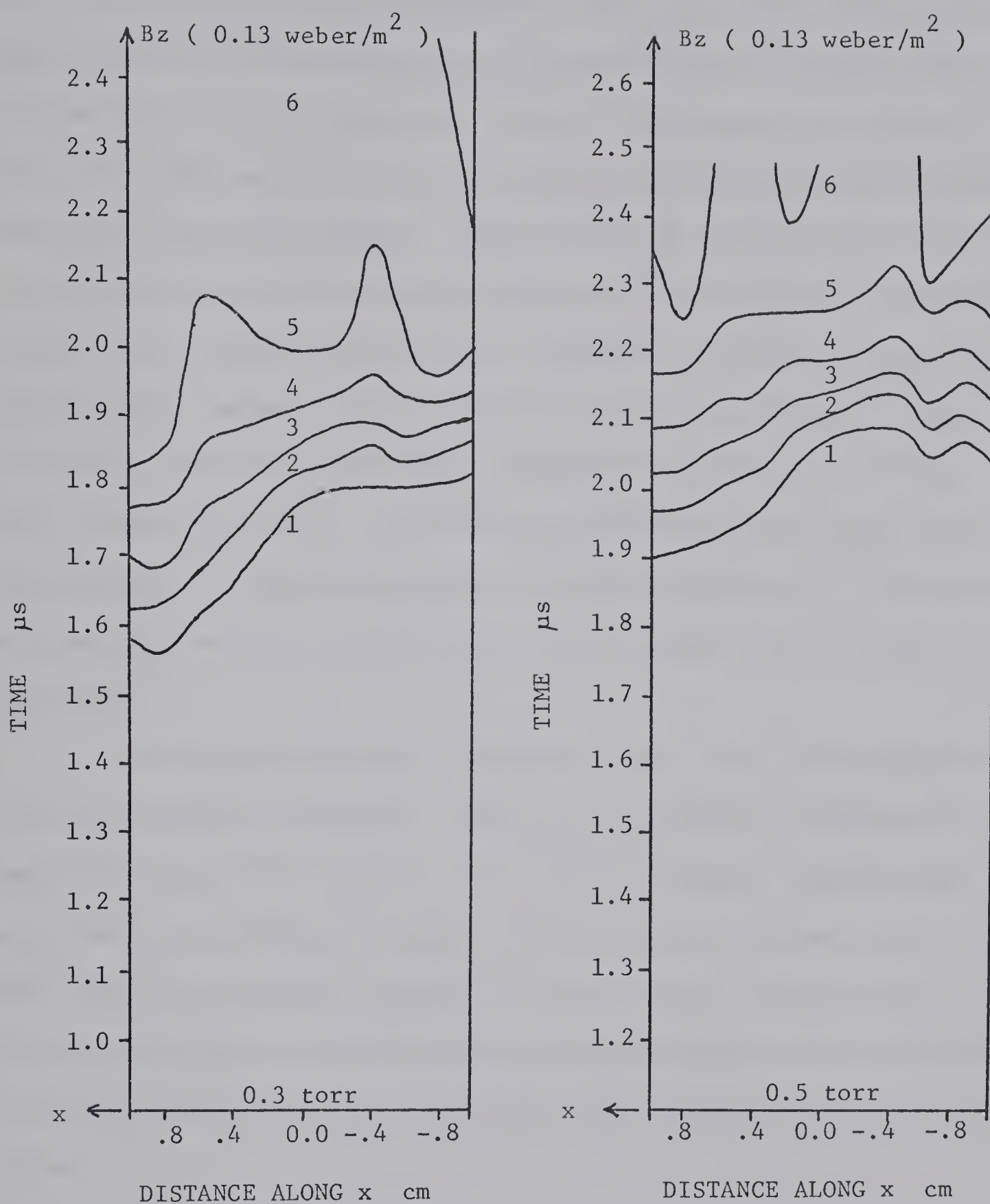


Figure 4.7 Nitrogen magnetic induction profiles.

listed in table 4.1 was measured in the region of highest current density in the current sheet near the anode [that is $x > 0$]. Thus the tilt angle recorded is the maximum tilt of the 0.39 weber/m^2 profile line over the upper half of the current sheet. In nitrogen at 0.3 and 0.5 torr it was much easier to specify a tilt angle for the current sheets since they were almost planar. These helium and nitrogen tilt angles are comparable to those reported by Johannson⁹ for argon and hydrogen. Similar to his findings there was no systematic variation in tilt angle with pressure changes. In both helium and nitrogen the current sheet having the least tilt in the region described above was the current sheet at lowest pressure. As pressure increased the tilt angle increased then decreased. Unlike the results reported for hydrogen^{3,4}, there was no transition between a perpendicular and a tilted sheet in this pressure range.

In helium the current density was from 2 to 3 times greater at the cathode than at the anode. There was a progressive increase in current density near the cathode [$x \approx -0.8$] as pressure was increased. As can be seen in figures 4.4 and 4.5 the current sheet was wider at the anode than at the cathode. Figures 4.4 and 4.5 also show that the current in the rear portion of the sheet does not go directly to the cathode but travels through the gas near the cathode back towards the back-plate of the gun.

The same concentration of current near the cathode was evident in nitrogen at 0.07 and 0.1 torr near the cathode. But the variation between anode and cathode was not quite as strong as that in helium. However, at pressures of 0.3 and 0.5 torr the current sheets

were almost planar with little variation in current density with changes of x . Current travelling parallel to the electrodes was also noticed in nitrogen at 0.07 and 0.1 torr as indicated in figure 4.6., but no such current was evident in figure 4.7 for 0.3 and 0.5 torr of nitrogen.

Unlike Lovberg⁵, who found the magnetic induction behind the current sheet to be constant, the magnetic induction was 33% more at $y = -3$ than $y = 0$ in helium and 25% larger in nitrogen. This fact was observed from the magnetic induction signals used to obtain current sheet velocities. This seems to indicate the current sheets can not be considered to be efficient pistons sweeping up all the gas in their path. However, this extra current flowing behind the current sheet could be carried by material ablated off the back-plate of the gun. One monolayer from the back-plate would be sufficient to carry this amount of current during the traversal of a current sheet down the gun. A substantial amount of material was eroded from the back-plate after many firings of the accelerator implying that this material was available to carry the extra current. If this was the case then the current sheet could be considered to be an efficient piston as noted by other authors^{3,5,6,8}.

Electric field strength, E_y , was plotted in the $x - t$ frame in order to determine the accelerating mechanism for the ions in the current sheet. Figures 4.8 to 4.11 show these profiles. Unlike most authors but similar to Pert's observation⁴ there was a region in the current sheet where E_y was negative. The reason for the occurrence of this negative axial field region is not known.

It is generally assumed that for electrons, in current sheets,

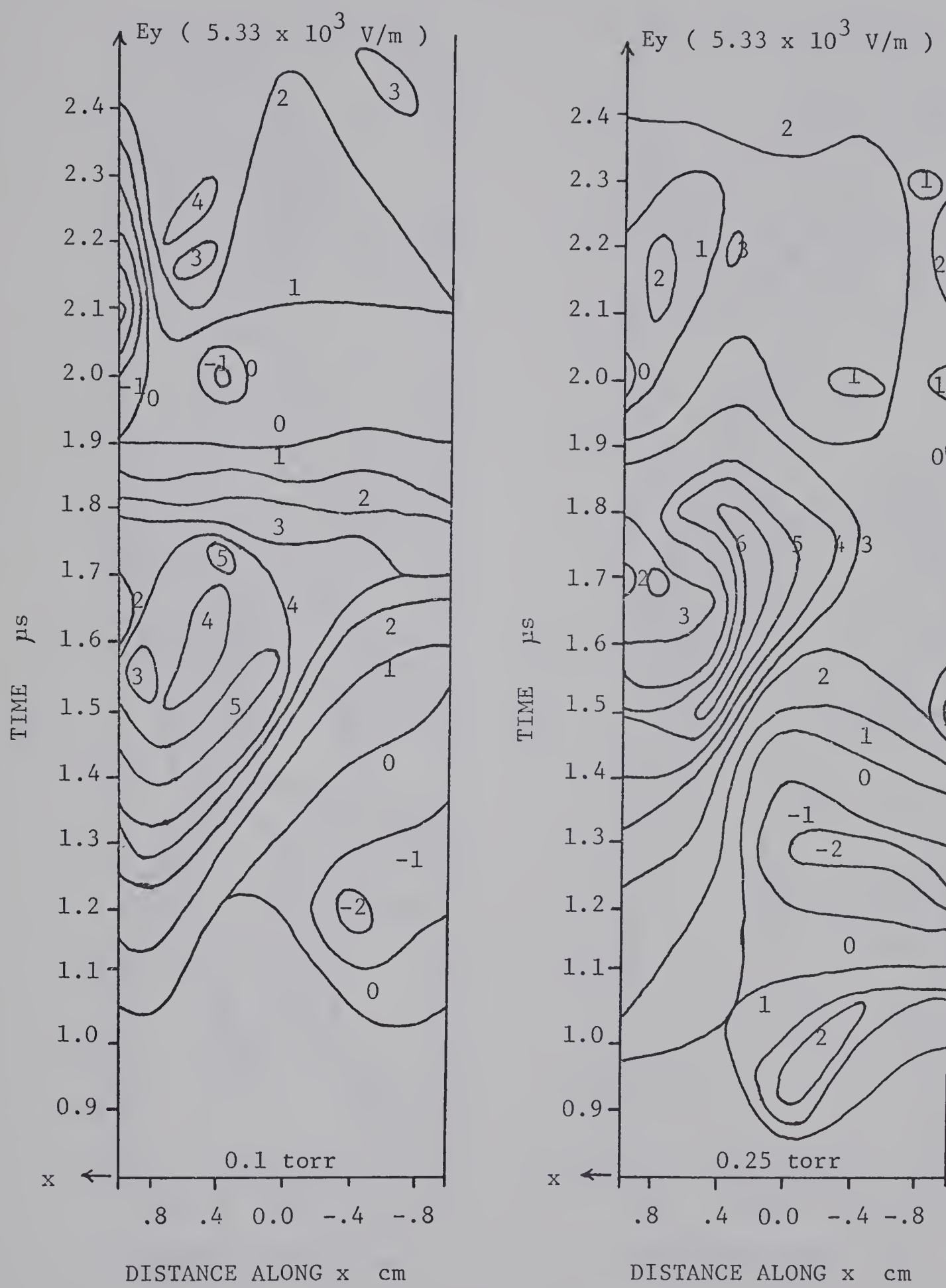


Figure 4.8 Helium electric field strength profiles.

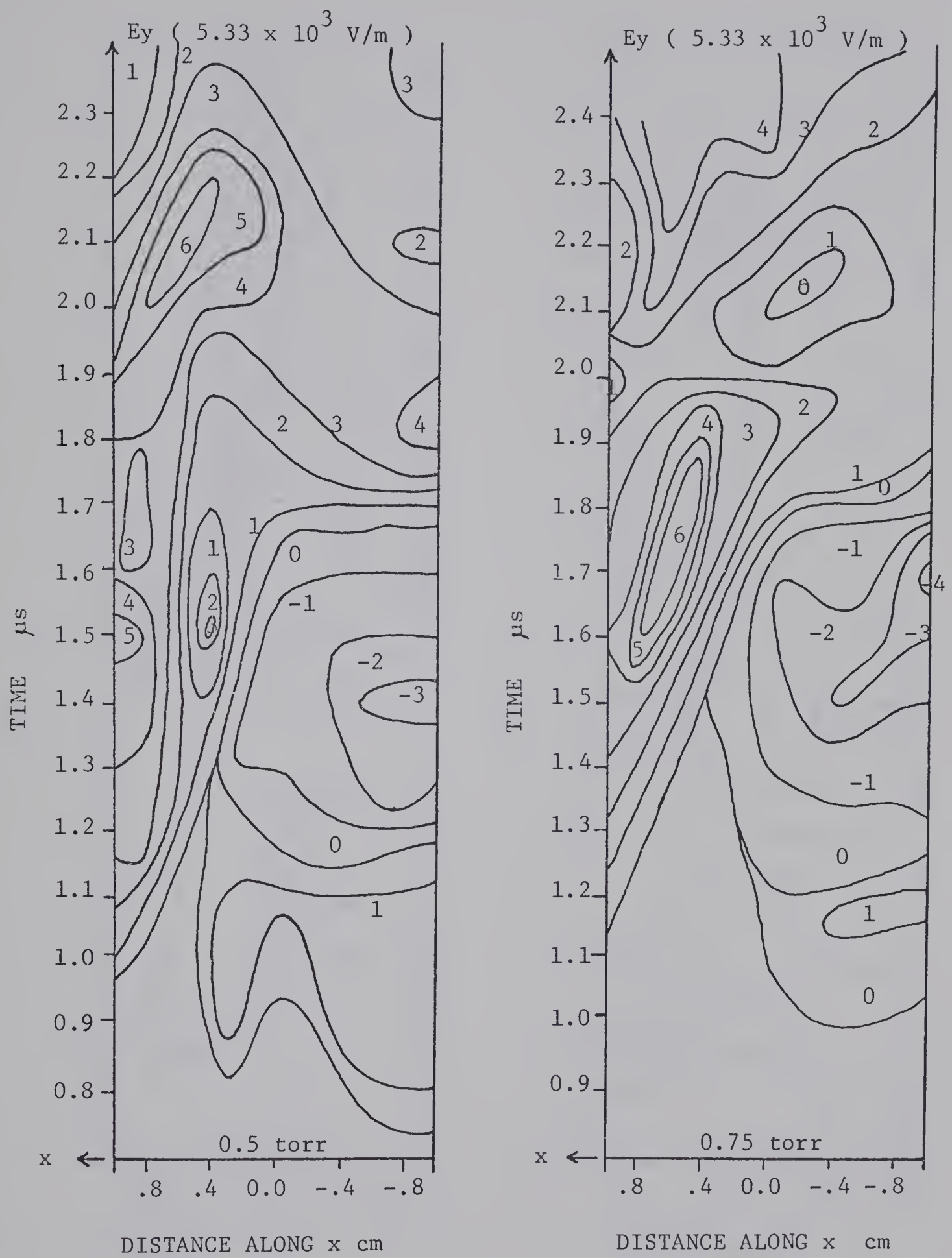


Figure 4.9 Helium electric field strength profiles.

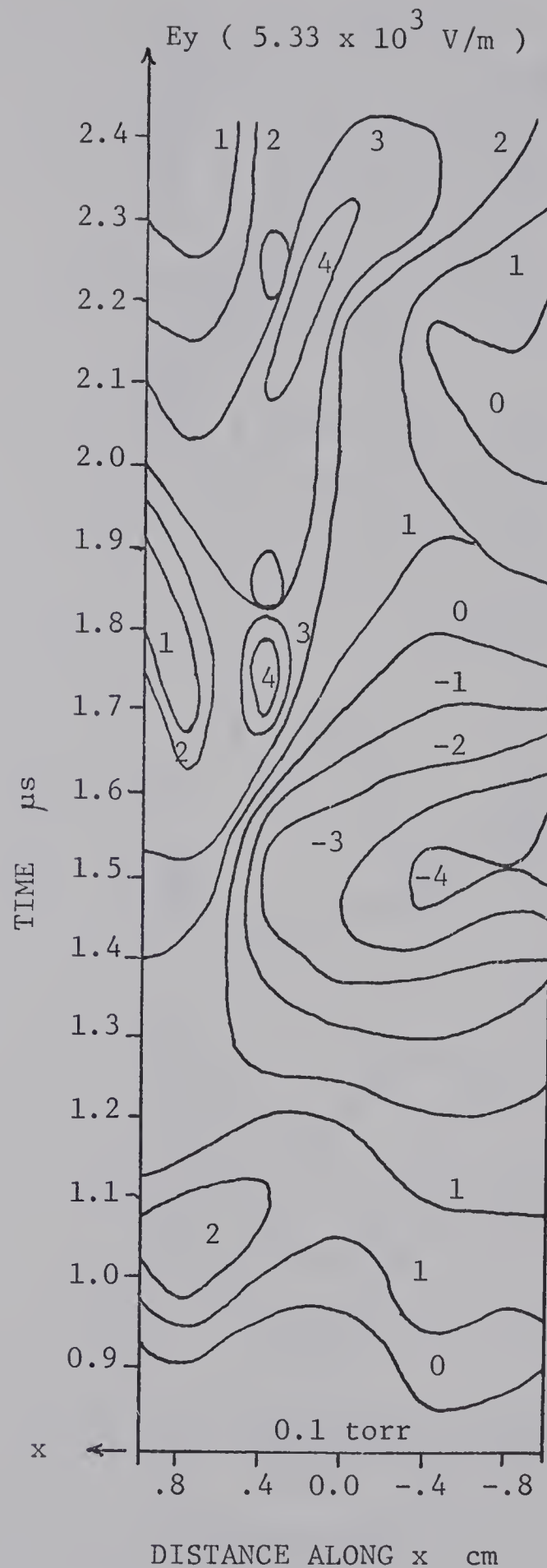
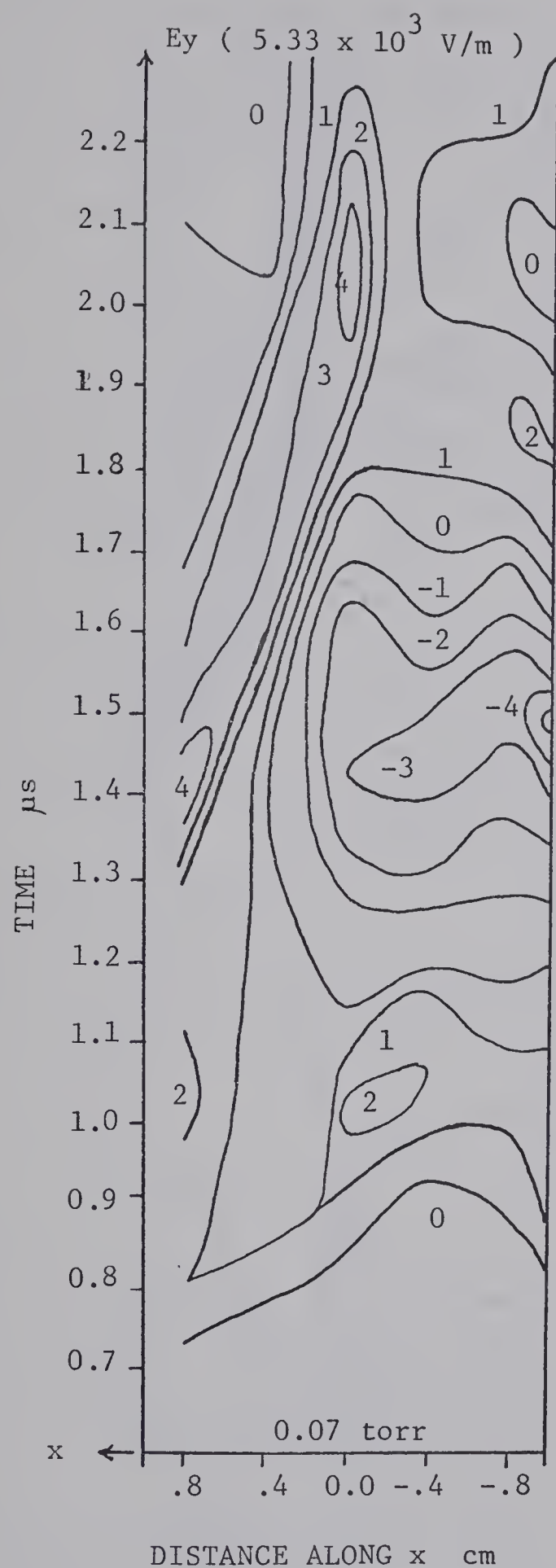


Figure 4.10 Nitrogen electric field strength profiles.

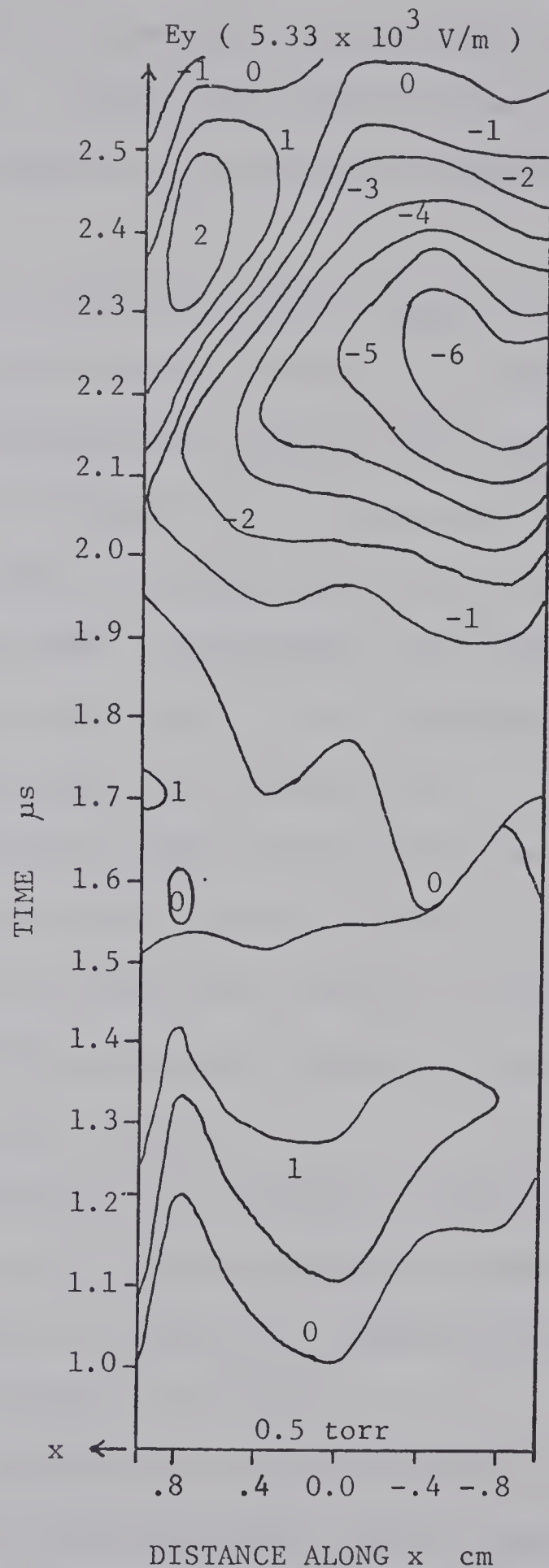
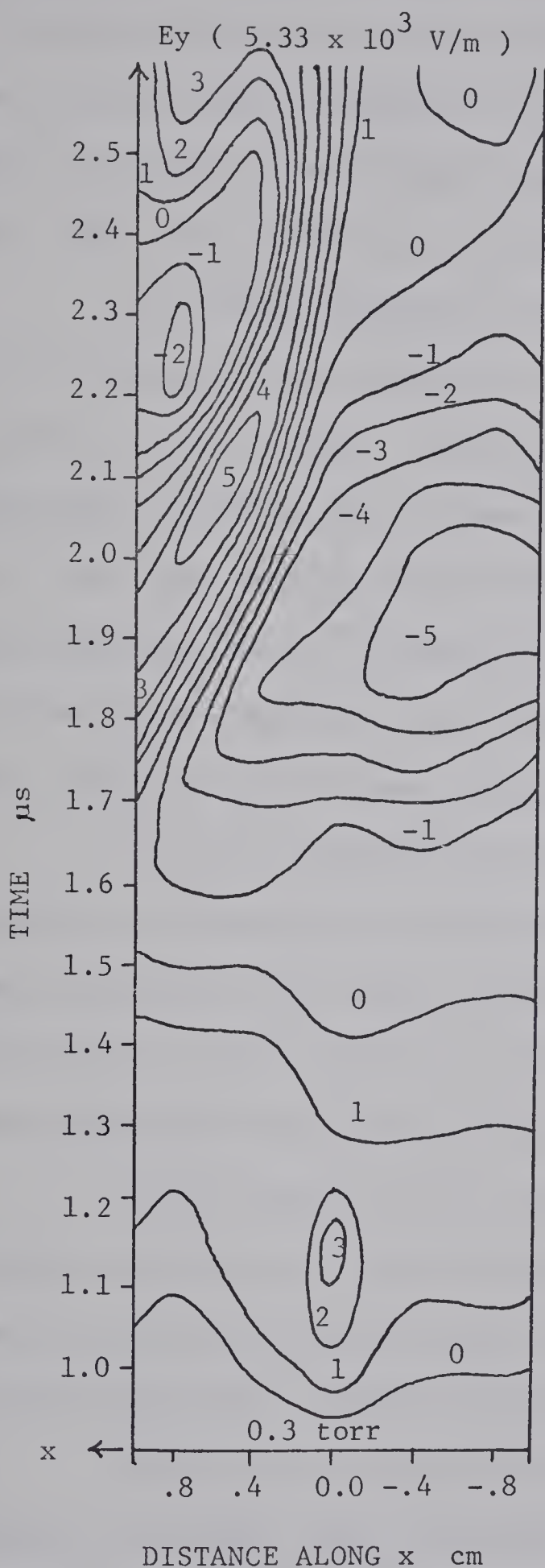


Figure 4.11 Nitrogen electric field strength profiles.

$w_{be} t_{ce} > 1$ thus the electrons would move in an $\underline{E} \times \underline{B}$ drift^{3,9}. When E_y is negative this $\underline{E} \times \underline{B}$ drift is towards the cathode, thus the electrons so drifting create a negative current. In order for positive current to flow, ions must travel towards the cathode in these regions of negative E_y . Thus ions constitute a current.

In helium, figures 4.8 and 4.9 show the region of negative E_y to be quite small and located in the front portion of the current sheet adjacent to the cathode. As the gas pressure was increased this region increased, including more volume in the current sheet. Figures 4.10 and 4.11 show that this region was even larger in nitrogen and also increased with pressure until it extended to the anode. Accompanying the increase in area was an increase in magnitude as well. At 0.5 torr of nitrogen the current sheet was almost entirely covered by a negative E_y .

If it is assumed that this negative field retarded electron current, or alternatively, enhanced ion current then ion current was a small fraction of the total current at low pressures in helium but gradually built up with pressure until at high pressure in nitrogen ion current constituted the majority of the total current.

In the regions where E_y was positive the electrons carried the current and thus were accelerated by a $\underline{j} \times \underline{B}$ force and dragged the ions behind them with the space charge field E_y . Where E_y was negative, ions carried the current and were accelerated by a $\underline{j} \times \underline{B}$ force.

With regards to the tilting phenomenon it was noticed that, in general, in regions where the electric field strength was large, either positive or negative, the current sheet tended to be perpendicular to the electrodes. Consequently the electric field strength has an import-

ant effect on the current sheet tilt, though the detailed mechanism by which this occurs is presently unknown.

CHAPTER 5

CONCLUSIONS AND SUGGESTIONS FOR FURTHER WORK

5.1 Conclusions

Current sheet tilt is not an obvious function of gas pressure. There was no monotonic increase or decrease with pressure changes, instead the tilt angle increased, then decreased, as pressure was increased.

The tilt of the current sheet may be linked with the axial electric field since the presence of a strong axial field corresponded to more perpendicular parts of the current sheet.

The axial electric field strength profiles were quite startling since a region of negative axial field was observed. This negative field adjacent to the cathode has not been previously charted. It will undoubtedly necessitate a major change in existing experimental models.

Current partitioning between ions and electrons varied with gas pressure and type. In helium at low pressure ions carried only a small fraction of the current in the sheet in a small region next to the cathode. As pressure was increased the ions carried more current until at 0.75 torr they carried almost all of the current in the lower half of the current sheet. The ions carried all of the current in the lower half of the current sheet in nitrogen at 0.07 torr and as pressure was increased up to 0.5 torr the ions carried almost all the current in the sheet.

5.2 Suggestions for further work

Upon observing the detailed profiles presented it can be seen that the tilting phenomenon is much more complex than it was originally thought to be. In order to solve this enigma, complete profiles will have to be obtained for electron, ion and neutral number density and temperature. When this is accomplished it should be possible to produce a mathematical model which will describe the microstructure of the current sheet and explain the tilting phenomenon.

APPENDIX A

MAGNETIC INDUCTION PROFILES

A.1 Current strip model

Magnetic induction in the current sheet is a direct consequence of current flowing in the plasma accelerator. A current sheet can be crudely represented by a collection of current strips as shown in figure A.1.

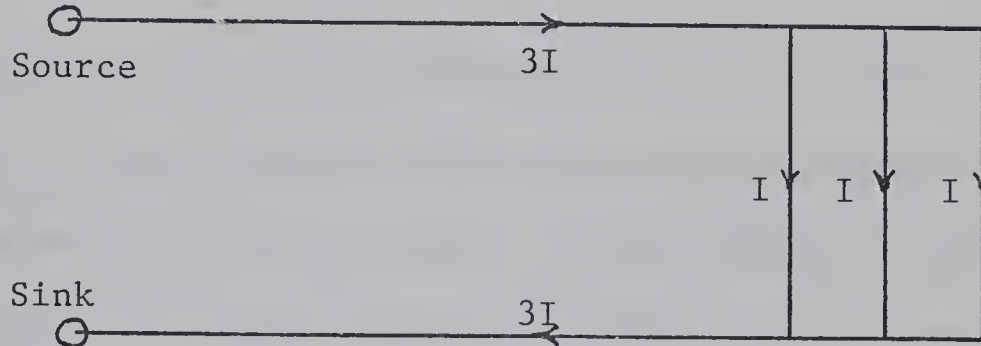


Figure A.1 Collection of current strips simulating a current sheet.

If this model is given the dimensions of the parallel plate plasma accelerator discussed in this thesis then the magnetic induction produced in this model should approximate that measured in the current sheet. To ensure that conditions are similar, the current strip model is assumed to be in motion so that the current strips pass an observation point 4.4 cm to the right of the stationary source. Thus the current strips are moving away from the current source. Assuming the current strips to be 8 cm wide, 2.4 cm long, and separated by 2 mm the magnetic

induction would be as shown in figure A.2.

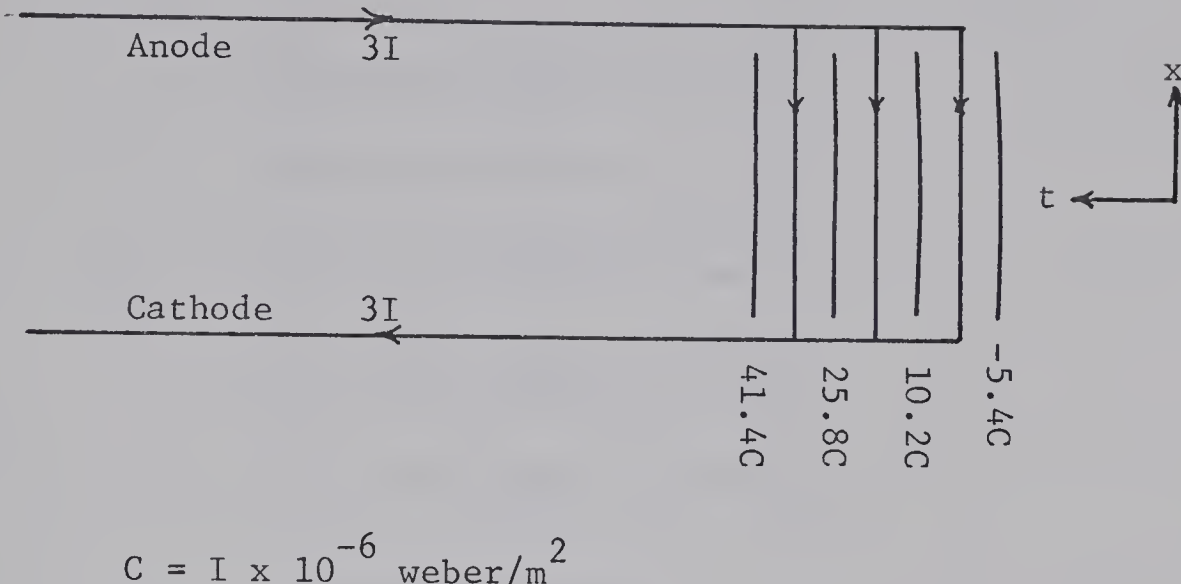


Figure A.2 Magnetic induction produced by current strips.

Profile lines indicate position of constant magnetic induction.

Now as indicated in figure A.2 the magnetic induction calculated is a function of time since the current path changes with time. The current strips have been superimposed on this x - t profile in order to indicate the position they occupied when each magnetic induction profile line was calculated.

Figure A.3 shows the same profile as figure A.2 with the current strips moving by the observation point at 2 cm/ μ s [t = 0 is arbitrary]. The magnetic induction lines are shown to be almost straight and perpendicular to the source and sink current strips. Thus if the current flowing in the current sheet is perpendicular to the accelerator electrodes the magnetic induction profile in the sheet should be perpendicular to the electrodes as this model indicates.

From the above discussion a typical magnetic induction trace measured from the current sheet would appear as in figure A.4. Oscillo-

scope traces were observed to have this form.

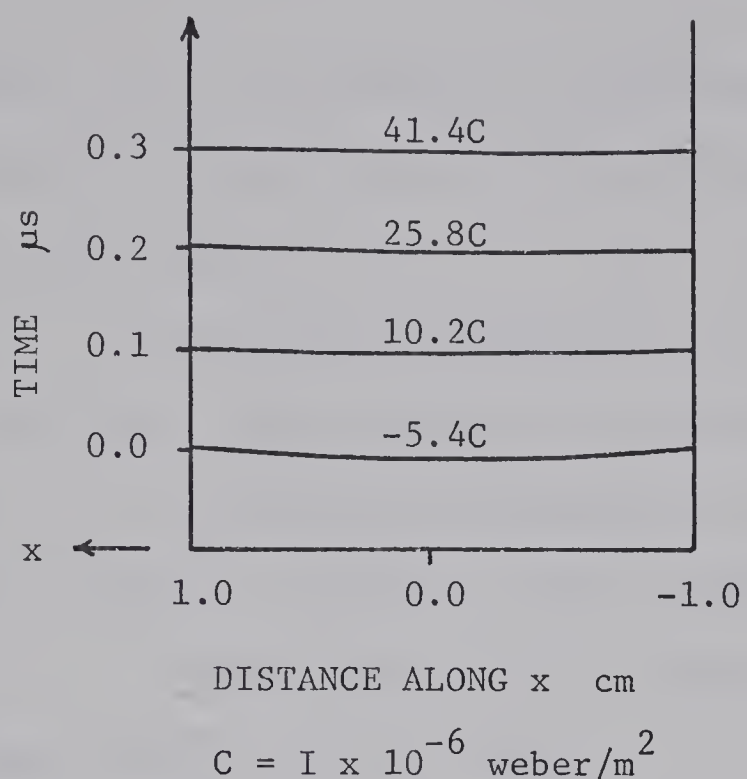


Figure A.3 Magnetic induction profile for current strip model.

Lines indicate position of constant magnetic induction.

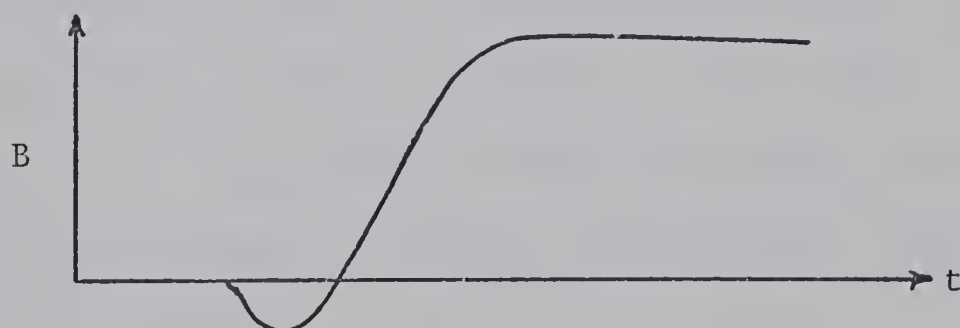


Figure A.4 Typical magnetic induction oscilloscope trace.

BIBLIOGRAPHY

- [1] Rosenbluth, M., in "A Symposium on Magnetohydrodynamics", [R. K. Landshoff editor], page 57, Stanford University Press, Stanford, [1957].
- [2] Pert, G. J., "Neutral-Gas Acceleration By an Electromagnetic Plasma Gun", Nuclear Fusion, 11, [1971].
- [3] Pert, G. J., "Current Sheet Structure in a Parallel-Plate Rail-Gun", Physics of Fluids, 8, 2185, [1970].
- [4] Pert, G. J., "Current Sheet Tilt in a Parallel-Plate Rail-Gun", Plasma Physics, 13, 63, [1971].
- [5] Lovberg, R. H., "Acceleration of Plasma By Displacement Currents Resulting From Ionization", VI International Conference on Ionization Phenomena in Gases, Paper IX 6, 235, [1963].
- [6] Lovberg, R. H., "The Measurement of Plasma Density in a Rail Accelerator By Means of Schlieren Photography", IEEE Transactions on Nuclear Science, 1, 187, [1964].
- [7] Lovberg, R. H., "Inferences of Plasma Parameters From Measurements of E and B Fields in a Coaxial Accelerator", Physics of Fluids, 7, S 57, [1964].
- [8] Burton, R. L. and R. G. Jahn, "Acceleration of Plasma By a Propogating Current Sheet", Physics of Fluids, 6, 1231, [1968].
- [9] Johansson, R. B., "Current Sheet Tilt in a Radial Magnetic Shock Tube", Physics of Fluids, 5, 866, [1965].

- [10] Khizhnyak, N. A. and A. A. Kalmykov, "Current Sheet Dynamics and Acceleration of Plasma in Electrodynamic Rail Accelerators", Soviet Physics - Technical Physics, 11, 1199, [1967].
- [11] Kulinski, S., "Interaction of Charged Particles With Moving Current Layer", Physics of Fluids Research Notes, 1133, [1967].
- [12] Pert, G. J., "A Model of an Ionizing Current Sheet", Journal of Physics A : General Physics, 3, 421, [1970].
- [13] Pert, G. J., "Structure of a Singly Ionizing Current Sheet Propagating in a Low Density Gas", Canadian Journal of Physics, 48, 1769, [1970].
- [14] Kvartskhava, I. F., Yu. V. Matveev, R. D. Meladze, E. Yu. Khautier, N. G. Reshetnyak, N. N. Zhukov, and A. D. Sinyavskii, "Possible Reasons For the Effect of Electrode Polarity on Rail Gun Acceleration of Plasma", Soviet Physics - Technical Physics, 4, 561, [1966].

B30012